Electronic Supplementary Material (ESI) for Physical Chemistry Chemical Physics.
This journal is © the Owner Societies 2024

# The Effect of Intermolecular Electronic Coupling on the Exciton Dynamics in Perylene Red Nanoparticles

C. Rehhagen, S. R. Rather, K. N. Schwarz, G. D. Scholes and S. Lochbrunner

## Supplementary Information

## Content

Supplementary Information - The Effect of Intermolecular Electronic Coupling on Exciton Dynamics in Perylene Red Nanoparticles

C. Rehhagen, S. Rafiq, K. N. Schwarz, G. D. Scholes and S. Lochbrunner

# 1. Experimental Details on the Spectroelectrochemical Measurements

For spectroelectrochemical measurements we apply a BASi EC Epsilon EClipse potentiostat in combination with an Agilent 8453 UV/vis spectrophotometer in a nitrogen filled glovebox. A Pine Research spectroelectrochemistry cell with a platinum honeycomb working electrode, platinum counter electrode, and an Ag/AgCl reference electrode is used. It is placed in a quartz cuvette with a pathlength of 1.7 mm. $Bu_4NPF_6$ with a concentration of 0.1 M in DMF is used as electrolyte solution.

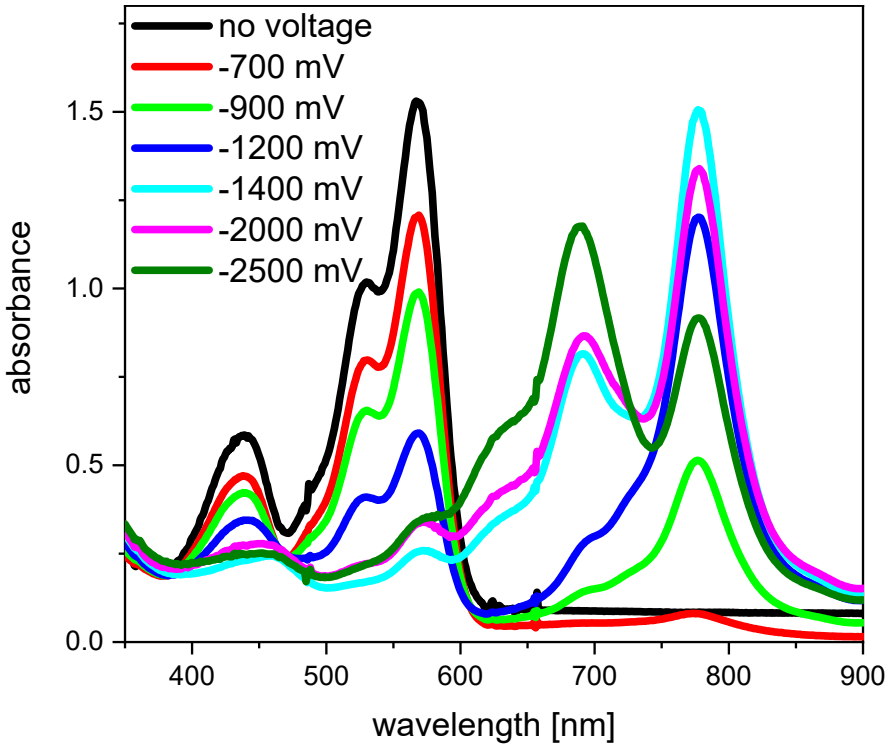


**Figure SI 1.** Absorption spectra of a PR/THF solution for different electrode potentials as described in the text.

Without an applied voltage we see the absorption of PR in THF. For intermediate voltages between -700 mV and -1200 mV a band at 780 nm increases with rising absolute voltage. We attribute this feature to the absorption of the anionic molecule. Increasing the absolute voltage further leads to the formation of a third contribution at about 700 nm, which we assign to the absorption of the doubly ionized anionic molecule.

## 2. Determination of Exciton Densities

For the determination of the exciton density, we make use of our information about excitation power, excitation spectrum, repetition rate (1 kHz), pump focus size (about 490 µm x 410 µm FWHM), probe focus size (about 125 µm x 65 µm), thickness of the cuvette (2 mm), concentration of the sample and its absorption spectrum.

We use the images of the pump, see Figure SI 2, and the pump power to calculate the fluence. The overlap of fluence and probe is optimized numerically to obtain the probed fluence distribution and thus the probed excitation photon distribution. Then, the absorption spectrum of the sample is weighted with the pump spectrum, see Figure SI 3. The pump-weighted absorption is used to determine the number of absorbed photons. With the concentration of the PR molecules in the sample we get the relative exciton density $n_{rel}$, i.e. average number of excitons per molecule.

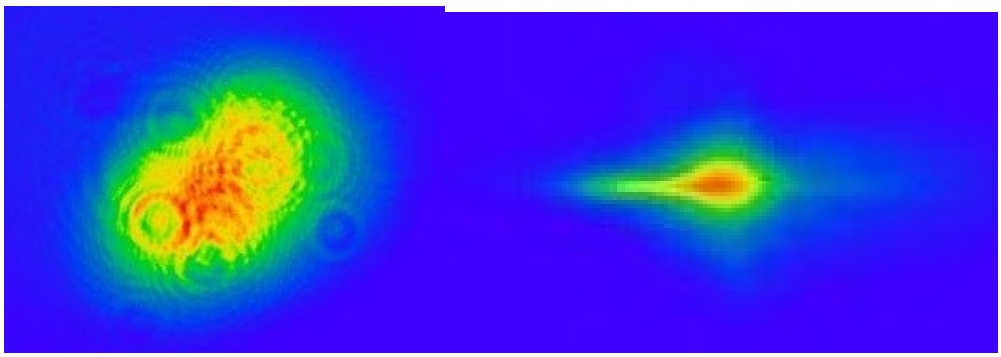

**Figure SI 2.** Image of the pump (left panel, 1.3 mm image width) and the probe (right panel, 0.656 mm image width) in the focal plane. The diffraction rings in the left panel result from attenuation filters used for adapting the pump power to the sensitivity of the camera.

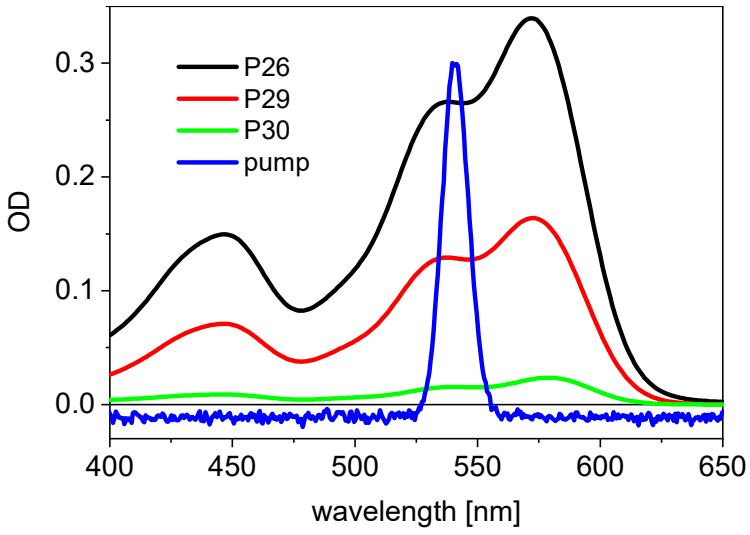


**Figure SI 3.** Absorption spectra of the samples used for the TA measurements and pump spectrum. The pump is artificially shifted along the y-axis for reasons of presentation, only. P26 is the sample with strong coupling and larger particles, P29 with strong coupling and smaller particles and P30 with weak coupling.

The determined exciton densities are not free of errors. We checked the consistency of the results by plotting the determined exciton densities versus the signal strength directly after the excitation pulse. A linear dependence is expected and also observed for the majority of the data. We performed a linear fit to the data and corrected then the deviating exciton densities by adjusting them to values

predicted by the linear fit. Please find an example of the basis for the correction in Figure SI 4 and the final values for all samples in Table SI 1.

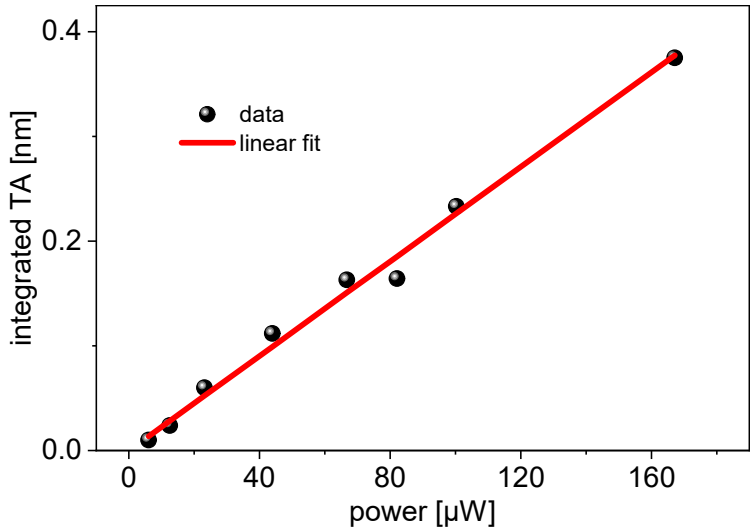


**Figure SI 4.** Integrated transient absorption between 550 and 650 nm depending on the excitation power of the experiment on P26, i.e., with strong coupling. The linear fit is used to correct the exciton density.

**Table SI 1.** Relative exciton densities of all TA experiments on nanoparticle systems. $n_{rel}$ is the relative exciton density. It is calculated as described in the text and corrected according to the fit in Figure SI 4.

| P26, i.e. with strong coupling | | | P29, i.e. strong coupling but small particles | | | P30, i.e. with weak coupling | | |
|---|---|---|---|---|---|---|---|---|
| P in µW | $n_{rel}$ calculated in % | $n_{rel}$ corrected in % | P in µW | $n_{rel}$ calculated in % | $n_{rel}$ corrected in % | P in µW | $n_{rel}$ calculated in % | $n_{rel}$ corrected in % |
| 6.0 | 0.0690 | 0.06 | 10.41 | 0.12 | 0.17 | 12.3 | 0.13 | 0.12 |
| 12.5 | 0.1440 | 0.12 | 22.7 | 0.26 | 0.26 | 78.5 | 0.828 | 0.78 |
| 23.2 | 0.2680 | 0.31 | 51.3 | 0.59 | 0.60 | 118.0 | 1.245 | 1.13 |
| 43.9 | 0.5070 | 0.57 | 66.6 | 0.77 | 0.76 | 164.0 | 1.73 | 1.84 |
| 66.8 | 0.7710 | 0.83 | 81.2 | 0.95 | 0.94 | - | - | - |
| 82.1 | 0.9490 | 0.84 | 106.8 | 1.23 | 1.05 | - | - | - |
| 100.3 | 1.1580 | 1.19 | 157.8 | 1.82 | 2.71 | - | - | - |
| 167.2 | 1.9300 | 1.92* | - | - | - | - | - | - |

* This value is adapted for the annihilation fit, since it expects it to be 2.1.

# 3. SEM-Images

The size distribution of the NP samples was characterized with dynamic light scattering (DLS) and also by scanning electron microscopy (SEM). A few drops of the nanoparticle suspension are dried on a SEM-sample holder and the sample is sputtered with 3 nm layer of iridium.

We do not find nanoparticles in the SEM images of the P30 sample, i.e. with weak coupling. This is probably due to the low concentration. Nevertheless, there are nanoparticles in the solution since they are detected in the DLS measurement, the quantum yield is significantly reduced, PR is insoluble in water and we observe the same processes in the TA measurements and the DAS analysis as in the other samples.

The size distribution given in the main manuscript is determined by measuring the size of about 2,000 single nanoparticles in the SEM images. The resolution is 4.88 nm corresponding to the size of one detector pixel.

These measurements were done in the Princeton Imaging and Analysis Center by C.R..

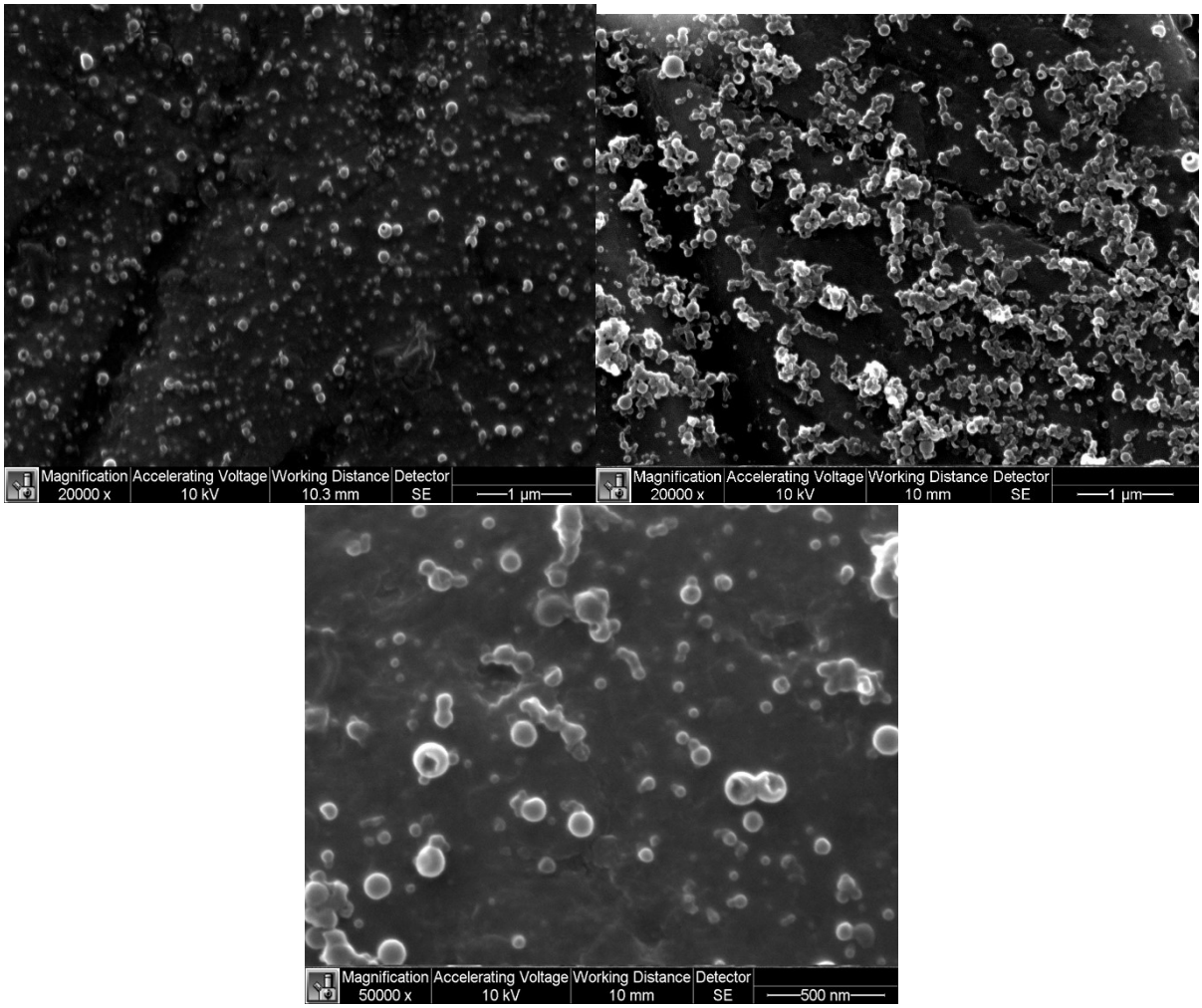


**Figure SI 5.** SEM images of P26, i.e. with strong coupling.

# 4. Static Absorption and Emission Spectra

## 4.1 Absorption Spectra Measured in Transmission

Upon formation of NPs, the spectra are slightly shifted to longer wavelengths and the second vibronic band gains intensity as the comparison to a THF solution of PR shows.

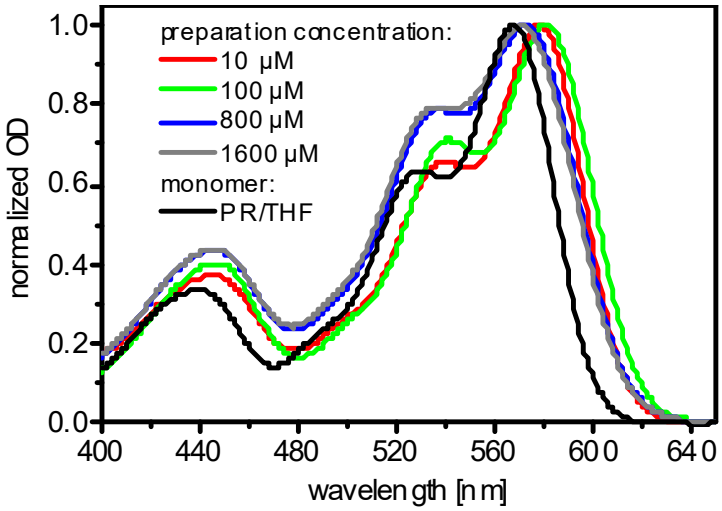


**Figure SI 6.** Normalized absorption spectra depending on the preparation concentration.

## 4.2 Absorption Spectra with Integrating Sphere

We find that the reshaping of the vibrational progression is not due to scattering effects since there should be a difference in the absorption spectra measured with and without an integrating sphere. In our samples, there is no such difference, see Figure SI 7.

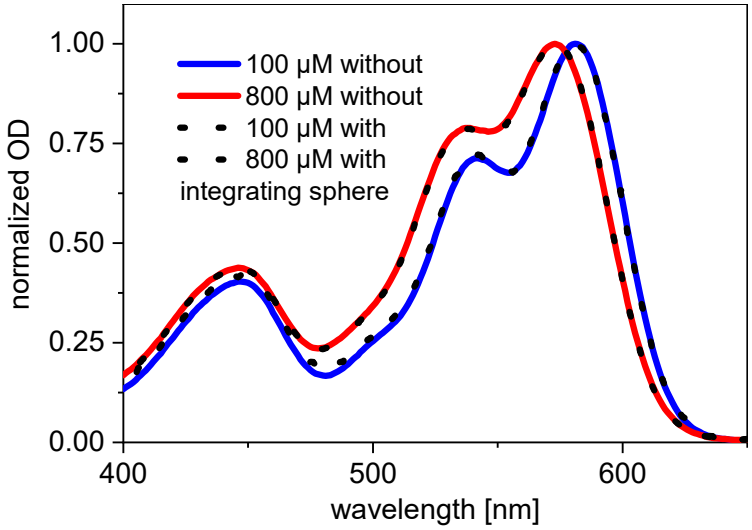


**Figure SI 7.** Absorption spectra with and without using an integrating sphere.

## 4.3 Emission Spectra

As in the absorption spectra, the NPs emission spectra are shifted to longer wavelengths upon NP formation.

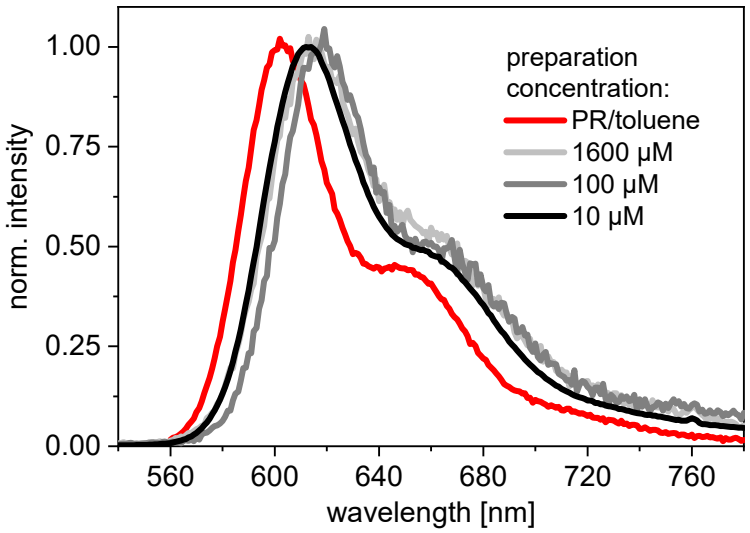


**Figure SI 8.** Normalized emission spectra depending on the preparation concentration. The nanoparticle samples are excited at 507 nm and the monomer sample at 540 nm.

# 5. Time-Resolved Emission

## 5.1 Experimental Details on Time-Correlated Single Photon Counting

The temporal decay of the emission was characterized by time-correlated single photon counting. In all measurements the measurement time lasted until an integrated peak intensity of 50,000 counts was reached. The excitation power is not high enough to observe any two-exciton effects. This is proven by two subsequent measurements on the same sample but with a factor of two in the excitation power. There are no differences in the results.

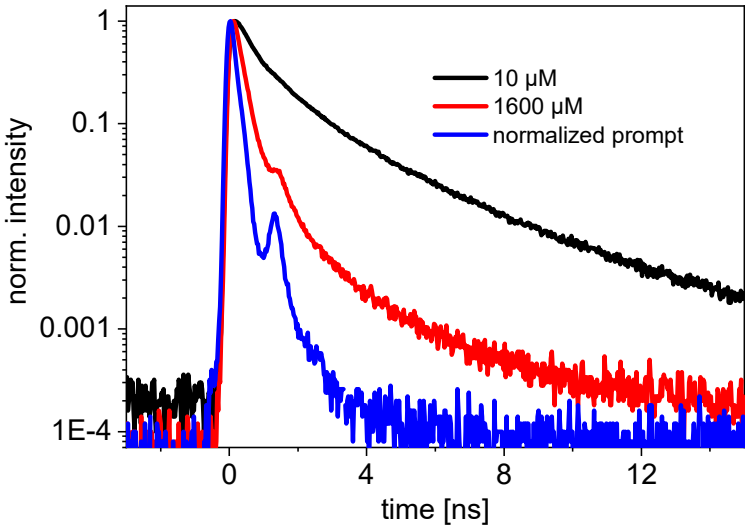


**Figure SI 9.** Time-Correlated Single Photon counting on NP samples with different preparation concentrations. The samples are excited at 507 nm. The peaks at 1.5 ns results from the shape of the prompt, see the instrument response function labelled as prompt response.

## 5.2 Additional Data of the Streak-Camera Measurements

For selected samples the emission was also characterized by streak camera measurements. A full data set for the sample P26 can be seen in Figure SI 10 and the spectra integrated over an early and a late time window compared to the static emission in Figure SI 11. We do not find any spectral dependence of the decay and there seem to be no other emissive species than the singlet excitons.

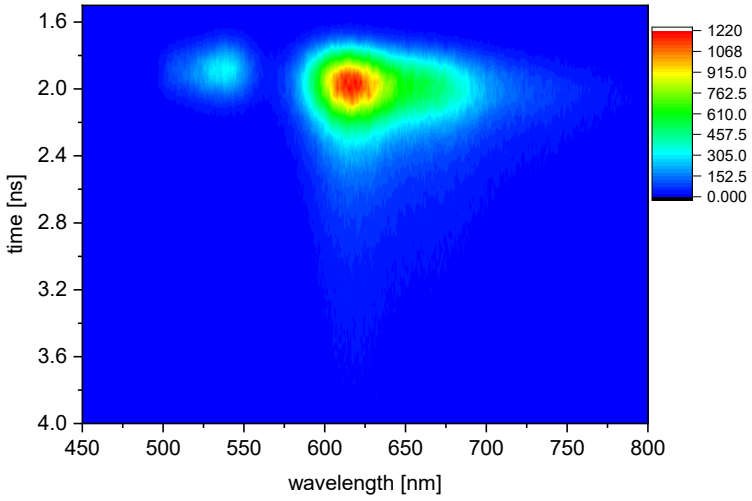


**Figure SI 10.** Full Streak Camera data. The peak at 540 nm is the scattered excitation light.

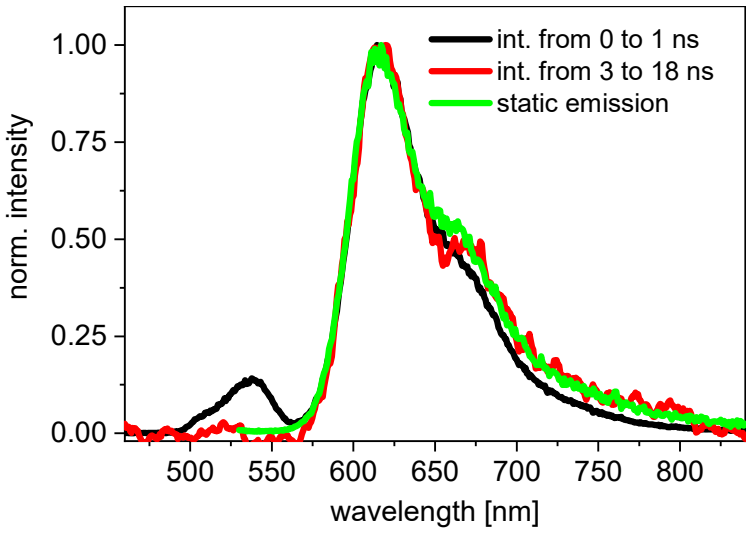


**Figure SI 11.** Integrated streak camera spectra compared with the static emission spectrum. The peak at 540 nm results from the scattered excitation light.

# 6. Transient Absorption Spectroscopy on Monomeric PR in THF

Transient absorption spectroscopy on PR monomers in THF at low exciton densities reveal that in contrast to the nanoparticles there are only contributions of GSB, SE and the ESA, see Figure SI 12. After a few picoseconds, the shape of the spectra does not change any more, see Figure SI 13, and the overall signal decays exponentially with a lifetime of about 5.9 ns, see Figure SI 14. There seem to be no other states than the first singlet excited state and the ground state involved.

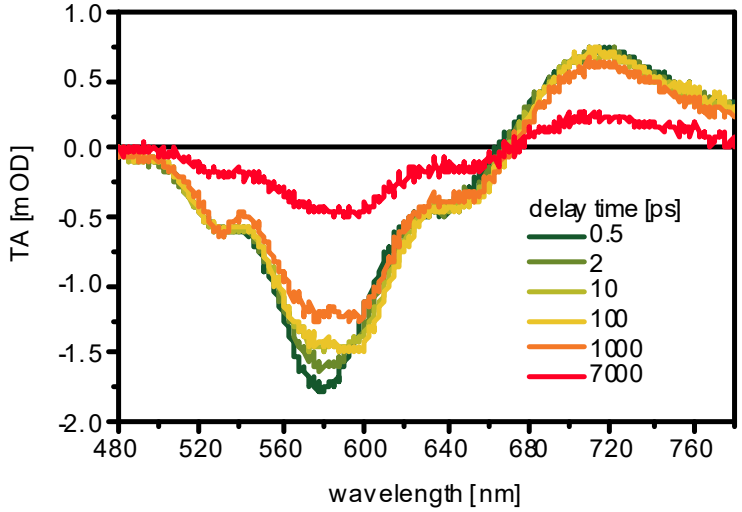


**Figure SI 12.** Transient spectra of PR in THF at low exciton densities.

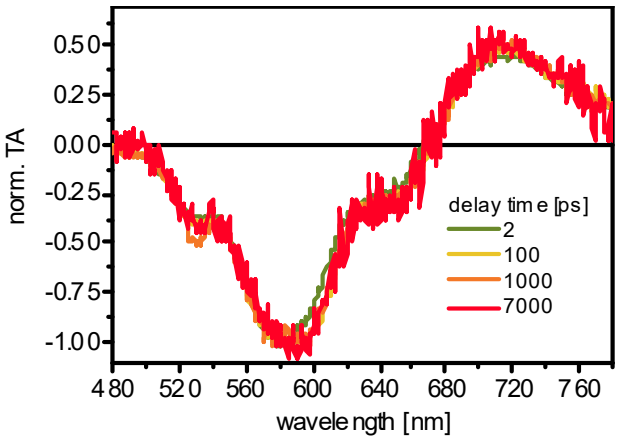


**Figure SI 13.** Normalized transient spectra of PR in THF at low exciton densities.

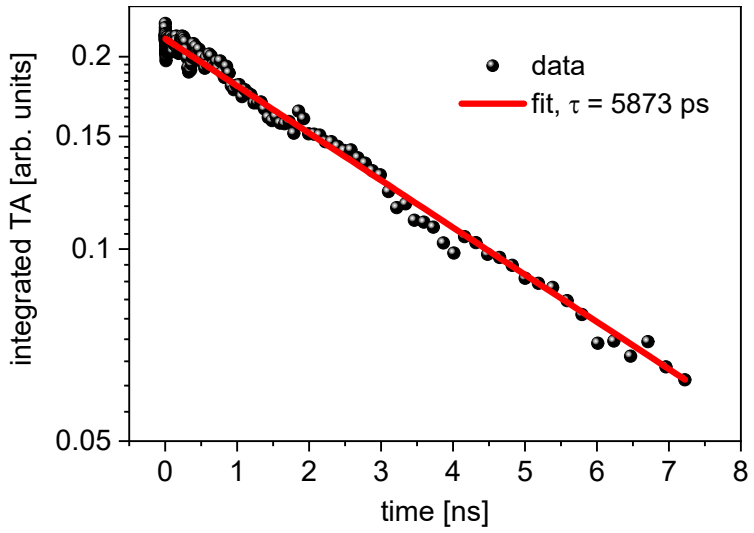


**Figure SI 14.** Transient signal of PR in THF at low exciton densities, spectrally integrated from 500 to 660 nm, and an exponential fit with a lifetime of 5873 ps.

# 7. Additional material on the transient absorption of the strong coupling system at low excitation power

In Figure SI 15 the decay of the transient signal of the strong coupling system is shown for different wavelengths. See Figure 5 in the main manuscript for the full transient spectra. The lifetime of the SE is 90 ps, the same time constant holds for the formation of the ISA component visible as an increase of the signal at 760 nm until a delay time of about 90 ps. The GSB and the ISA decay within 1100 ps. Please note, that although the components dominate at the given wavelengths, they still overlap and influence also the signal characteristic of the other.

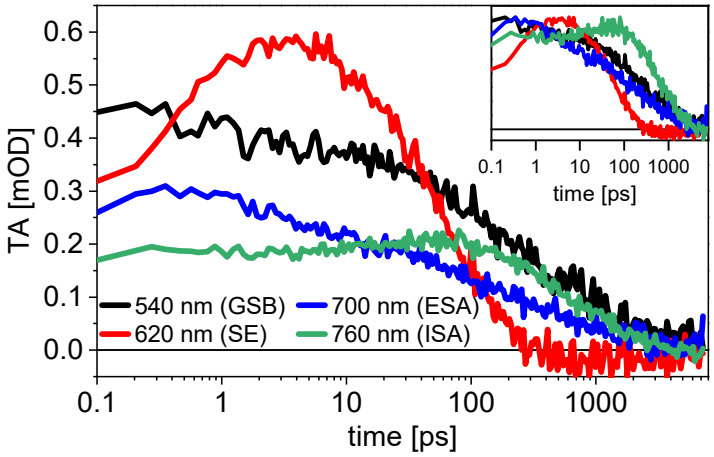


**Figure SI 15.** Decay of the transient signal of the strong coupling system as described in the main manuscript at different wavelengths. The wavelengths are chosen such the transient signal is dominated by the component given in the brackets of the legend. In the inset, the same decays are normalized to a maximum value of 1.

Figure SI 16 shows all decay associated spectra of the strong coupling system at low excitation power.

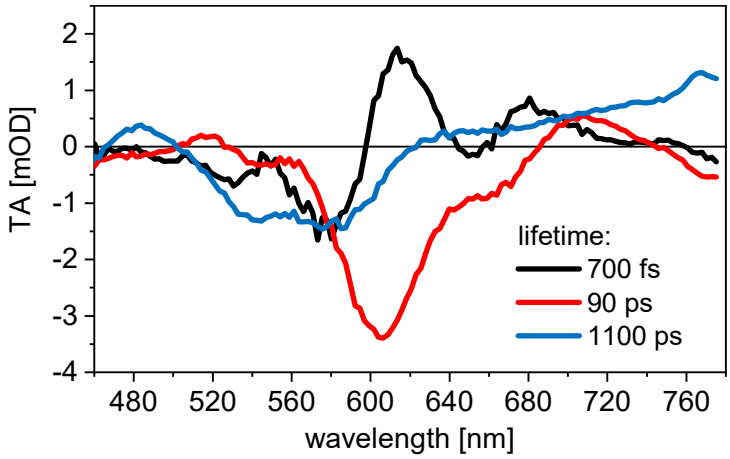


**Figure SI 16.** Decay associated spectra of the transient absorption of the strong coupling system at low excitation power.

# 8. Transient Absorption Spectra of the weak coupling NP system

The transient absorption of the weak coupling system is measured as described in the main manuscript. The DAS look almost identical to those of the strong coupling sample. There are differences in the region dominated by the GSB. We attribute this to the different shape of the absorption spectra due to the difference in the coupling, see Figure SI 6.

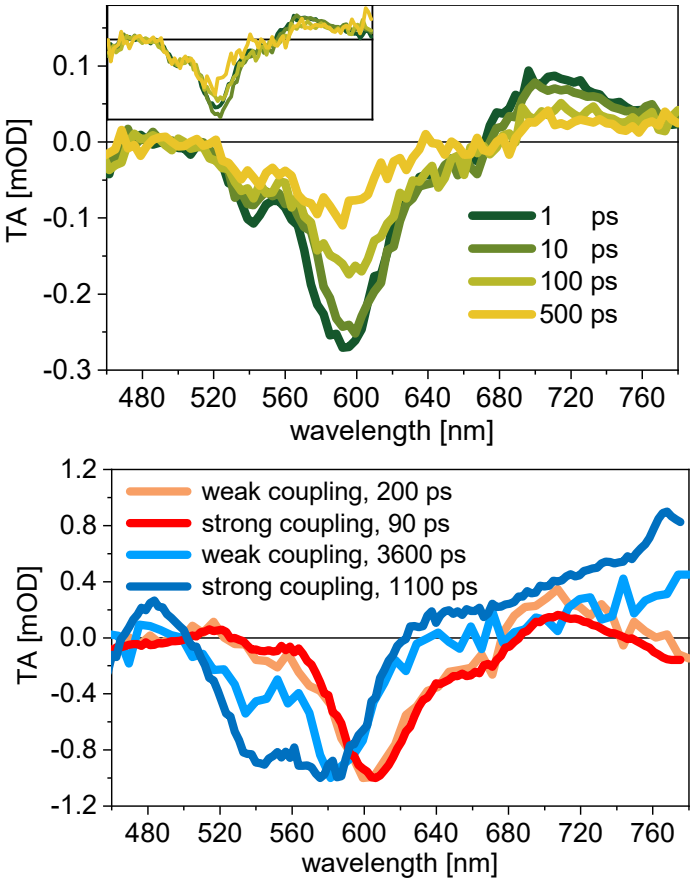


**Figure SI 17.** Transient absorption spectra of the NPs with weak coupling (upper panel). The inset shows the spectra normalized to the signal at 550 nm. DAS of the NPs with strong and weak coupling (lower panel).

# 9. Transient Absorption Spectroscopy at High Exciton Densities on the Weak Coupling NP System

The decay of the excited state species in the system with weak coupling accelerates with increasing exciton density, see Figure SI 18, but the effect is much weaker than in the strong coupling system. See the main manuscript for the transient spectra.

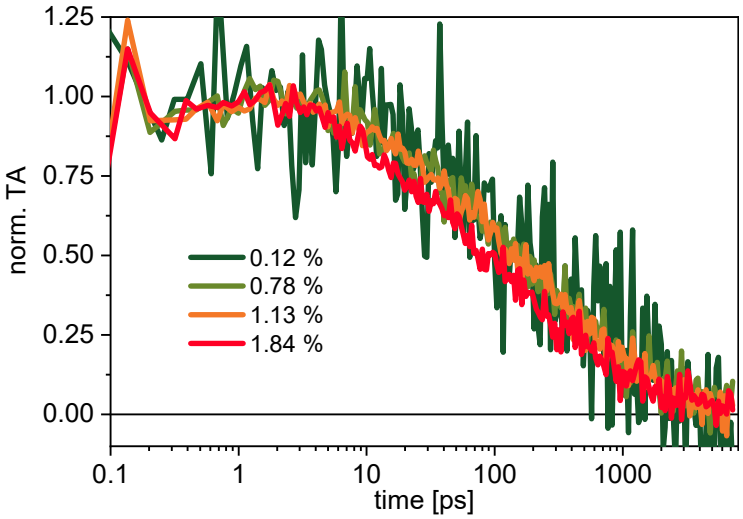


**Figure SI 18.** Acceleration of the decay at 600 nm in the system with weak coupling. The legend gives the number ratio of excited and unexcited molecules.

# 10. Determination of the Exciton Diffusion Constant

The exciton diffusion constant D is determined by numerically solving the differential equation E1 given in the main manuscript and fitting it to the data. We start with the calculated exciton densities and the lifetimes determined from the low excitation measurements. All measurements are fitted separately.

## 10.1 Large Particles with Strong Coupling

The results of the first fit iteration are shown in Table SI 2.

**Table SI 2.** Results of the first fitting iteration. D is the diffusion constant. Only D and the amplitudes of the EAS are fitted. The exciton density of the measurement marked by * is adapted from 1.9 % to 2.1 % in another run of the fitting procedure, since it further improves the quality of the fit. Then, the value with * reads 0.176.

| appr. excitation power in µW | D in $nm^2/ps$ |
|---|---|
| 6 | - 0.00068 |
| 12 | 0.023 |
| 23 | 0.11 |
| 44 | 0.149 |
| 67 | 0.155 |
| 100 | 0.156 |
| 160 | 0.184* |

At low excitation power, the results for the diffusion constant are not meaningful since the exciton density is too low for a significant contribution of annihilation. A diffusion constant of D = 0.166 $nm^2/ps$ in combination with lifetimes of $\tau_1$ = 89 ps and $\tau_2$ = 1053 ps represents a good compromise of the obtained fit figures. Using this set of values results in fit curves which reproduce the data at all excitation levels very well, see Figure 7 of the main manuscript. The evolution associated spectra (EAS) of all fits are consistent as be seen from Figure SI 19 and Figure SI 20.

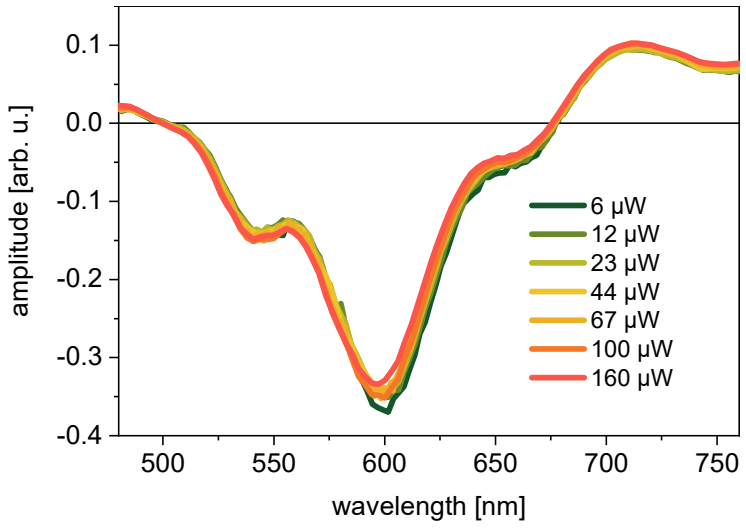


**Figure SI 19.** Evolution associated spectra (EAS) of the singlet state obtained for the different excitation powers, see legend. D is taken as 0.166 $nm^2/ps$ and the applied exciton densities are determined as described above. The amplitude is the only free parameter.

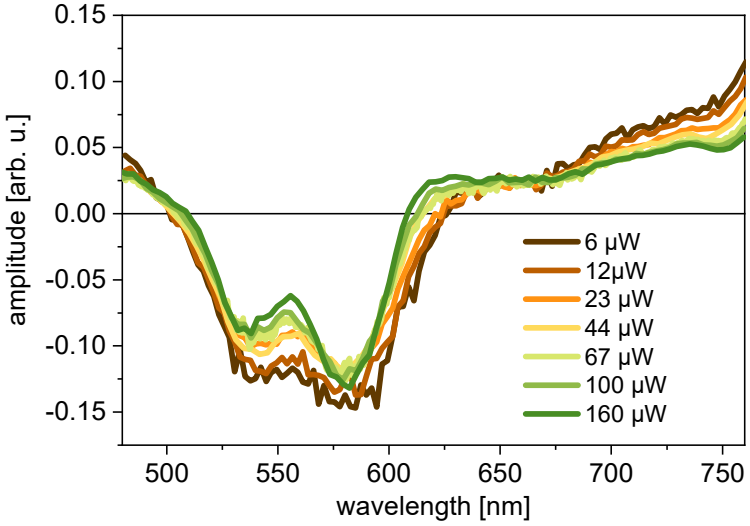


**Figure SI 20.** EAS of the intermediate state obtained for the different excitation powers, see legend. D is taken as 0.166 $nm^2/ps$ and the applied exciton densities are determined as described above. The amplitude is the only free parameter.

## 10.2 Particles with Weak Coupling

The same procedure as described above is performed. The results of the first fit iteration are listed in Table SI 3.

**Table SI 3.** Results of the first fitting iteration. D is the diffusion constant. Only D and the amplitudes of the EAS are fitted.

| appr. excitation power in µW | D in $nm^2/ps$ |
|---|---|
| 12 | 0.0639 |
| 79 | 0.0157 |
| 118 | 0.0157 |
| 164 | 0.0212 |

At the lowest excitation power, the results for the diffusion constant are not meaningful since the exciton density is too low for a significant contribution of annihilation. A diffusion constant D of 0.0182 $nm^2/ps$ in combination with lifetimes of $\tau_1$ =187 ps and $\tau_2$ = 3584 ps represents a good compromise of the obtained fit figures. Using this set of values results in fit curves which reproduce the data at all excitation levels very well. The evolution associated spectra (EAS) of all fits turn out to be consistent as demonstrated in Figure SI 21 and Figure SI 22. The model reproduces with the given numbers very well the time evolution of the singlet state as can be seen from the spectrally integrated stimulated emission, see Figure SI 23.

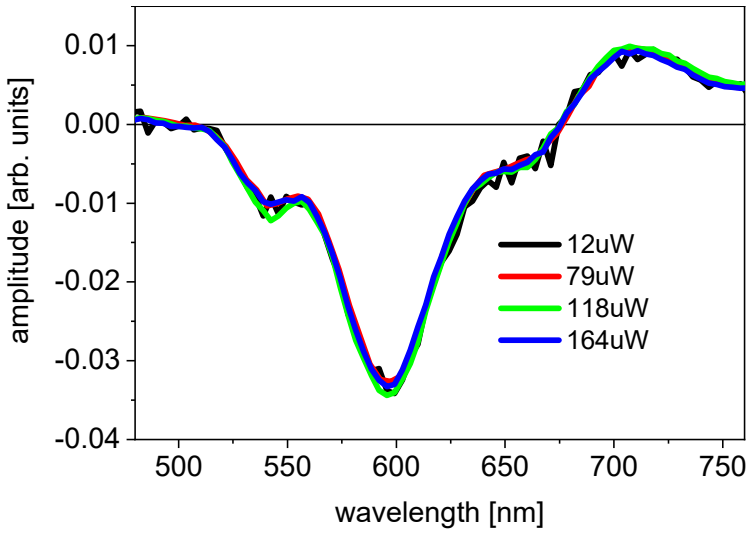


**Figure SI 21.** EAS of the singlet state in the weak coupling case obtained for the different excitation powers, see legend. D is taken as 0.0182 $nm^2/ps$ and the applied exciton densities are determined as described above. The amplitude is the only free parameter.

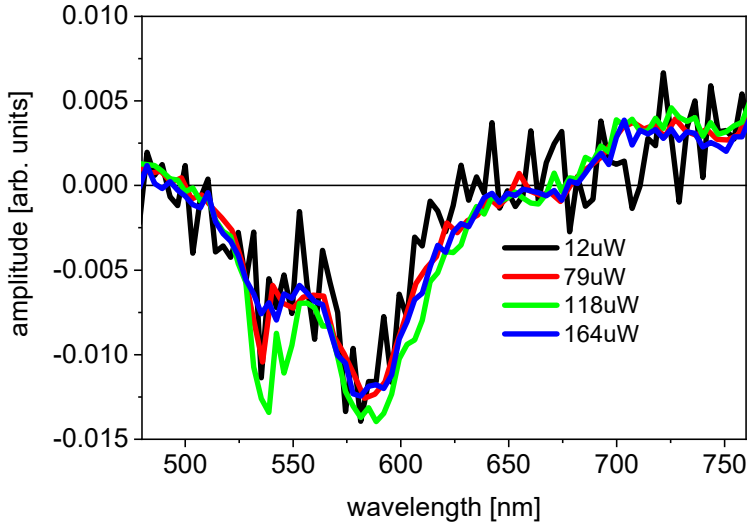


**Figure SI 22.** EAS of the intermediate state in the weak coupling case obtained for the different excitation powers, see legend. D is taken as 0.0182 $nm^2/ps$ and the applied exciton densities are determined as described above. The amplitude is the only free parameter.

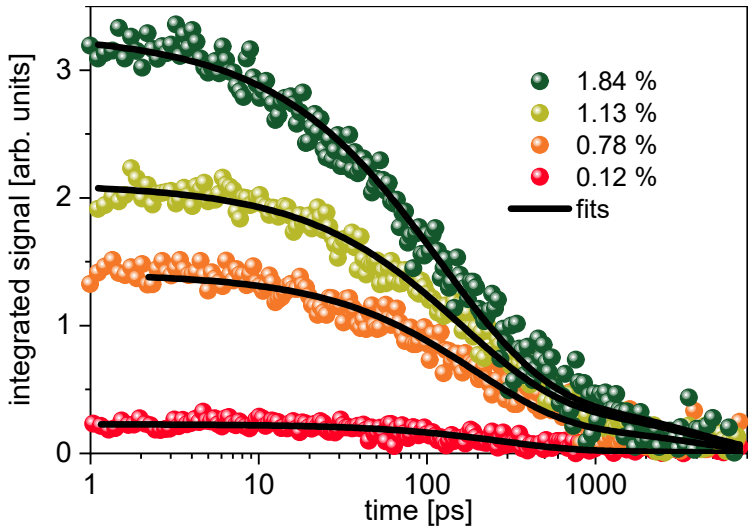


**Figure SI 23.** Integrated transient absorption signal of the SE spectral region, i.e. 610-650 nm, and the fitted model.

# 11. Spectral Overlap and Förster Transfer

In order to assess the influence of the various factors on the mobility of the singlet excitons, we calculate the spectral overlap S of absorption and emission defined as

$$S = \int OS(\nu)\nu^4 d\nu = \int \varepsilon(\nu)F(\nu)\nu^4 d\nu$$

with the overlap spectrum OS, the molar extinction coefficient ε and the fluorescence intensity F[2]. S(λ) is plotted in Figure SI 24. After integration of S(ν) over the wavenumber, the ratio of the two overlap integrals for weak and strong coupling is 1.14. Thus, the spectral overlap of the system with weak coupling is higher contrary to the exciton diffusion constant demonstrating that not the spectral overlap as described in [1] but the electronic coupling between the singlet sites is the key factor for the mobility of the excitons.

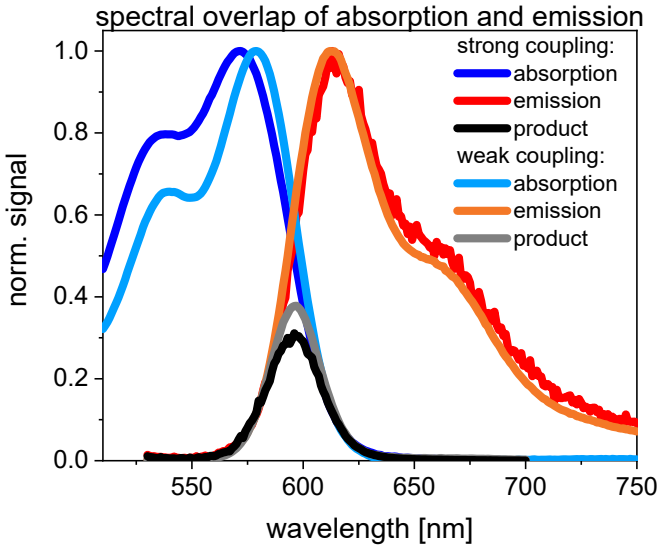


**Figure SI 24.** Absorption and emission spectra with strong and weak coupling and their spectral overlap $\varepsilon F\nu^4$.

# 12. Transient Absorption Spectroscopy on a Strong Coupling NP System with Small NPs

The sample is prepared with a precipitation concentration of 800 µM instead of 1600 µM as in the sample presented in the main manuscript. Within the experimental error, there are no differences in spectroscopic properties such as absorption and emission spectra and the quantum yield. According to DLS measurements, the average size of the nanoparticles is 50 nm in contrast to 90 nm found for the sample prepared with dye concentration of 1600 µM. Thus, the coupling conditions are comparable to those of the strong coupling system, but the size of the NPs is different.

TA experiments are performed as described in the main manuscript. Please find the exciton densities in Table SI 1 and the TA-spectra in Figure SI 25 and normalized to a common bleach in Figure SI 26.

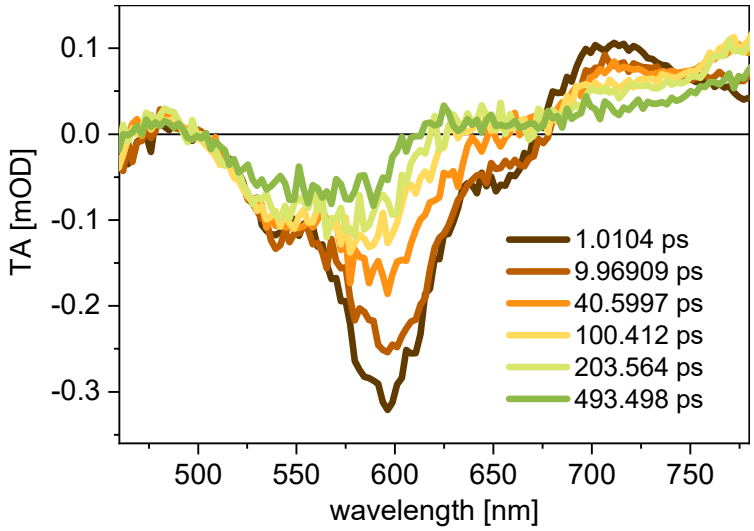


**Figure SI 25.** TA-spectra of NPs prepared with 800 µM dye concentration. Spectra are taken at a low exciton density, i.e. with an excitation power of 22 µW.

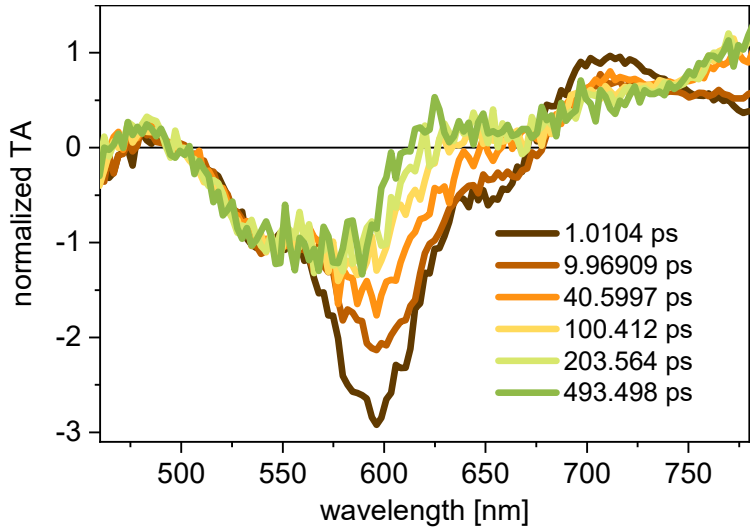


**Figure SI 26.** TA-spectra of NPs prepared with 800 µM dye concentration normalized to the signal at 550 nm.

The DAS and exponential decay times obtained by the fit are identical within the experimental error for both strong coupling systems, i.e. for the small and large particles, see Figure SI 27.

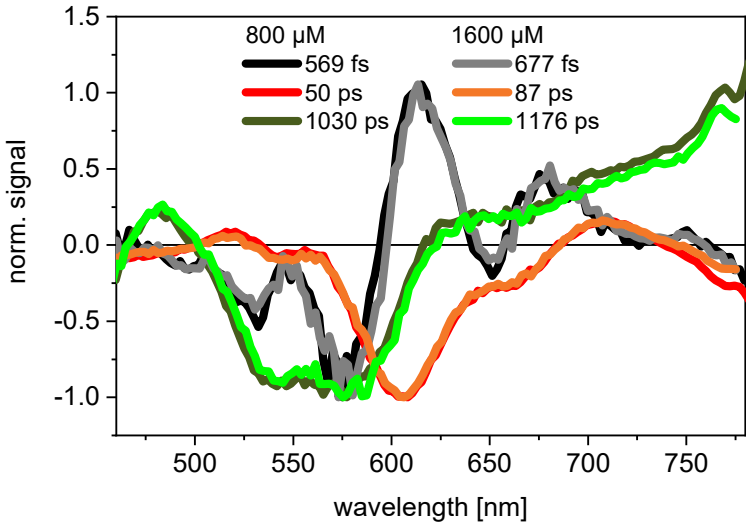


**Figure SI 27.** Normalized DAS of the NPs prepared from 800 µM and 1600 µM solutions.

We apply the exciton annihilation model described in the main manuscript to analyze the acceleration of the decay dynamics with excitation density.

The results of the fitting procedure for the exciton diffusion constants are given in Table SI 4. For a singlet lifetime of 50 ps, as determined by the global analysis at low exciton densities, the diffusion constant depends on the excitation power. At a singlet lifetime of 90 ps, this effect does not occur. We conclude, that 90 ps is a more realistic value for the singlet lifetime which is also in agreement with the quantum yield. We use D = 0.154 $nm^2/ps$, $\tau_1$ = 90 ps and $\tau_2$ = 1030 ps as final values. The fits are shown in Figure SI 28 and the EAS in Figure SI 29 and Figure SI 30. Our model describes the decay satisfactorily and all EAS' are consistent to each other.

**Table SI 4.** Results of the first fitting iteration. D is the diffusion constant. Only D and the EASs are fitted. The shorter lifetime is set to 90 ps instead of 50 ps as given in Figure SI 27. See the text for details.

| appr. excitation power in µW | D in $nm^2/ps$ |
|---|---|
| 50 | 0.146 |
| 67 | 0.149 |
| 80 | 0.146 |
| 108 | 0.149 |
| 158 | 0.178 |

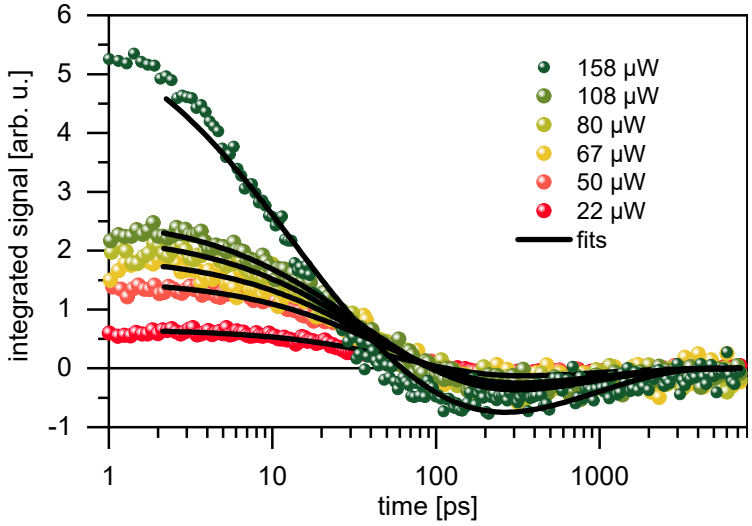


**Figure SI 28.** Integrated transient absorption signal in the spectral region of the SE, i.e. 610-650 nm, and the fitted model. Please see also the exciton densities given in Table SI 1, since the exciton densities are signal-corrected in contrast to the excitation power.

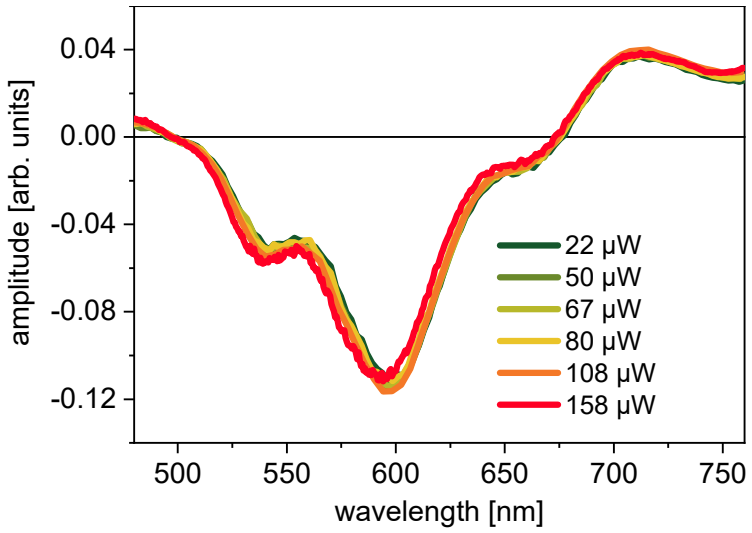


**Figure SI 29**. EAS of the singlet state for different excitation powers using D = 0.154 $nm^2/ps$, $\tau_1$ = 90 ps and $\tau_2$ = 1030 ps. The amplitude is the only free parameter.

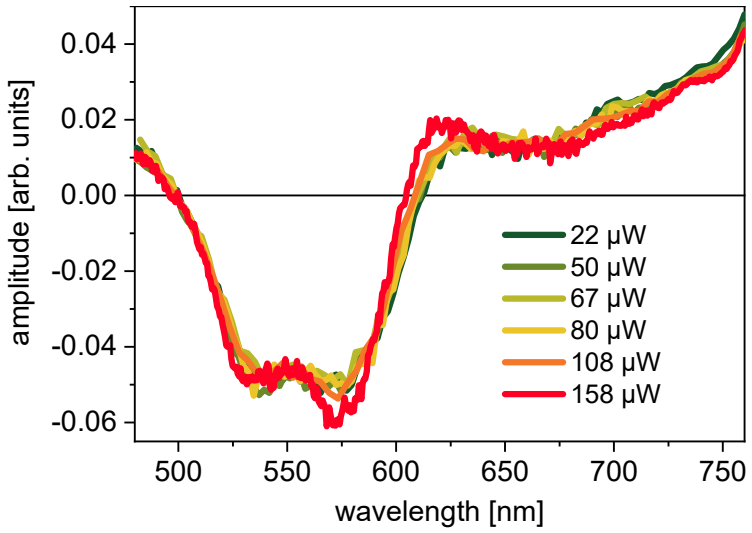


**Figure SI 30.** Evolution associated spectra of the intermediate state for different excitation powers using D = 0.154 $nm^2/ps$, $\tau_1$ = 90 ps and $\tau_2$ = 1030 ps. The amplitude is the only free parameter.

# 13. References

[1] Förster T 1948 Zwischenmolekulare Energiewanderung und Fluoreszenz *Ann. Phys.* **6/2** 55–75
[2] Haugland R P, Yguerabide J and Stryer L 1969 Dependence of the Kinetics of Singlet-Singlet Energy Transfer on Spectral Overlap *Proc. Natl. Acad. Sci.* **63** 23–30